

**PAPER • OPEN ACCESS**

## Effect of milling parameters on the dispersion characteristics of multi-walled carbon nanotubes in transition metal oxides

To cite this article: S S Lephuthing *et al* 2018 *IOP Conf. Ser.: Mater. Sci. Eng.* **430** 012002

View the [article online](#) for updates and enhancements.

**IOP | ebooks™**

Bringing you innovative digital publishing with leading voices to create your essential collection of books in STEM research.

Start exploring the [collection](#) - download the first chapter of every title for free.

# Effect of milling parameters on the dispersion characteristics of multi-walled carbon nanotubes in transition metal oxides

S S Lephuthing\*, A M Okoro, M Lesufi, O O Ige and P A Olubambi

Centre for Nanoengineering and Tribocorrosion, Department of Metallurgy, School of Mining, Metallurgy and Chemical Engineering, University of Johannesburg, Republic of South Africa

\*senzenil@uj.ac.za

**Abstract.** In this research investigation on milling parameters to achieve uniform dispersion of multi-walled carbon nanotubes (MWCNTs) was conducted. High-energy ball milling (HEBM) technique was adopted to disperse 1 wt. % MWCNTs in titanium and manganese oxides with ball to powder ratio (BPR) of 10:1 at 6 and 9 hours milling times. Scanning electron microscopy (SEM), transmission electron microscopy (TEM) and X-ray diffraction (XRD) were used to characterize the as-received MWCNTs and admixed composite powders. The results indicated that HEBM was an effective route to disperse MWCNTs in transition metal oxides. In addition, the characteristics of admixed powders evidently showed that the increase of milling time effectively dispersed the MWCNTs in titanium and manganese oxide respectively, however deformation of sidewalls of MWCNTs was observed due to harsh milling conditions that resulted on non-sp<sup>2</sup> defects in the MWCNTs.

## 1. Introduction

Owing to the unique chemical, thermal conductivity, physical and mechanical properties, carbon nanotubes (CNTs) have paved way on their applications as reinforcements in functional materials such as polymers, metals and transition metal oxides (TMOs) [1–3]. Transition metal oxides have been extensively studied as promising functional materials due to their potential application on catalysis, chemical sensors, and energy conversion/storage devices. However, they have drawbacks which are low thermal conductivity, brittle nature and low fracture toughness which have motivated researchers to employ strategies in reinforcing them [3,4]. In addition, MWCNTs are the best candidate to address the inherent limitations of TMOs as they exhibit excellent mechanical properties with Young's modulus and tensile strength in the range of 0.2-0.95 TPa (5 times stronger than stainless steel) and 11-150 GPa, respectively. Additionally, they undergo plastic deformation under severe bending stress conditions without showing brittle deformation behaviour [5].

Despite these exceptional properties that MWCNTs contribute to TMOs, an effective and efficient route on synthesis of TMOs/MWCNTs composite are yet to be fully established [3]. During the synthesis of TMOs/MWCNTs composites, there are challenges associated with achieving homogenous dispersion of MWCNTs in TMOs. These challenges are due to the nanoscale dimensions and strong van der Waals forces among individual tubes, which lead to the agglomeration of MWCNTs and minimises the total surface free energy that results in poor compatibility with TMOs components [3,6–8]. Various studies on dispersion techniques of MWCNTs in metals and TMOs [9–11] have been done;



liquid phase, electrochemical deposition, thermal deposition, and High-energy ball milling (HEBM) in a bid to achieve homogeneous dispersion of MWCNTs.

High energy ball milling is a widely used technique to disperse MWCNTs, despite the effectiveness of this technique, past works have revealed that MWCNTs are subjected to harsh milling conditions that may damage the MWCNTs and eventually make them lose their unique properties [12]. When MWCNTs are damaged during a milling operation, there are tendencies of introducing vacancies and imperfections in the C–C system with broken sp<sup>2</sup> bonds that may lead to formation of weak sp<sup>3</sup> C–C amorphous phase which initiate sites for interfacial reactions [13]. Nevertheless, MWCNTs exhibit a significant chemical stability because of the strong graphitic basal planes, which composed of strong sp<sup>2</sup> C–C bonds in the outer shell of the nanotubes [14]. Besides, when the outer layer become damaged unlike single walled carbon nanotubes (SWCNTs) that has single graphitic plane, the MWCNTs will still have other graphitic planes that will retain its unique properties in TMOs composites [15]. In this study, HEBM techniques were adopted with optimized milling parameters to disperse 1 wt. % MWCNTs in transition metal oxides and the dispersion characteristics of the MWCNTs were ascertain by using various advanced characterization facilities.

## 2. Materials and Methods

### 2.1. Starting materials

The starting powder materials used for this study were MWCNTs (NX7100- A -Ultra purified CNT) with average diameter of 9.5 nm and an average length of 1.5  $\mu\text{m}$ , supplied by Nanocyl, Belgium. Titanium (IV) anatase (TiO<sub>2</sub>) and manganese (IV) oxides (MnO<sub>2</sub>) powders were 99, 6 and 99.9 % at -325 mesh particle size respectively supplied by Industrial Analytical.

### 2.2. High energy ball mill (HEBM)

A high-energy ball mill (Retch 400, Germany) was used to disperse 1 vol. % MWCNTs into TiO<sub>2</sub>/MnO<sub>2</sub>. Dry milling was conducted by charging each TMO powder in a alumina vial (250 ml, inner diameter (ID) = 100 mm) with alumina balls of diameter 5 mm. Ball to powder ratio (BPR) was 10:1 at different time 6 and 9 hours at constant speed of 100 rpm with a relaxation time of 10 minutes, to prevent the samples from overheating. The admixed powders were collected and characterized after milling

### 2.3. Characterization of as received and admixed powders

Scanning electron microscopy (FESEM, Carl Zeiss Sigma) equipped with energy dispersive X-ray spectrometry (EDX) and transmission electron microscopy (JEOL-Jem 2100) were used for morphology characterisation of starting and admixed powders. X-ray diffractometer (XRD, Rigaku D/max-rB) was used for phase identification scanning using Cu-K  $\alpha$  ( $\lambda = 0.154$  nm) radiation at a scanning rate of 1  $^{\circ}$ /min over the angular range of 20–90  $^{\circ}$ .

## 3. Results and Discussion

### 3.1. Morphology of dispersed MWCNTs in titanium oxide and manganese oxide

Figure 1 shows the SEM and TEM images of as-received MWCNTs, TiO<sub>2</sub>/MnO<sub>2</sub>. The MWCNTs as shown are agglomerate into clusters due to the strong Van der Waal forces between individual MWCNTs. Achieving dispersion of MWCNTs in this transition metal oxide requires suitable milling parameters to de-entangle them by reducing the effects of the strong Van der Waal forces. TiO<sub>2</sub> particles are spherical shaped and MnO<sub>2</sub> particles exhibit amorphous irregular shapes of different granules

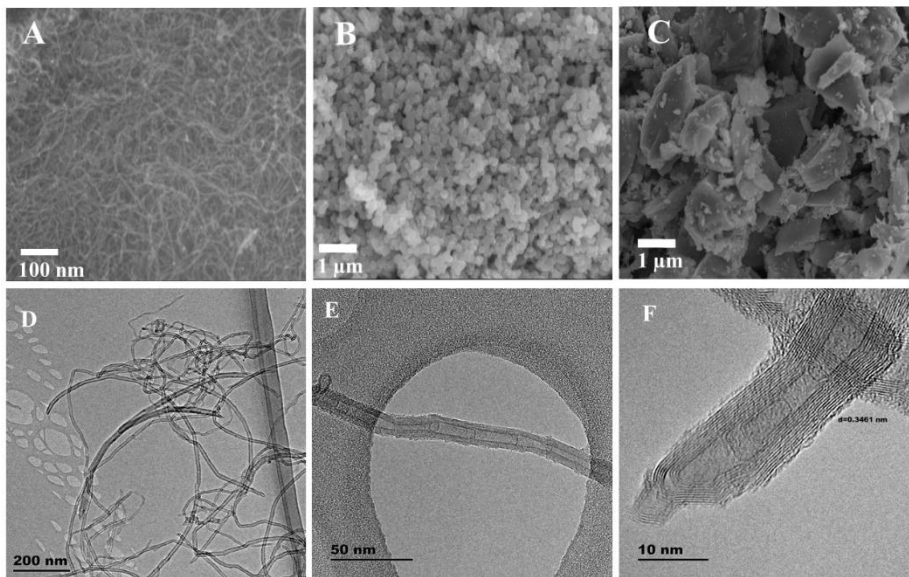


**Figure 1:** SEM and TEM images of the as-received powders A -MWCNTs, B -titanium oxide and C-manganese oxide, D-F indicates as-received powders MWCNTs (D) agglomerate of as received MWCNTs, (E) tubular structure of individual MWCNTs and (F) HRTEM image showing the individual walls of MWCNTs.

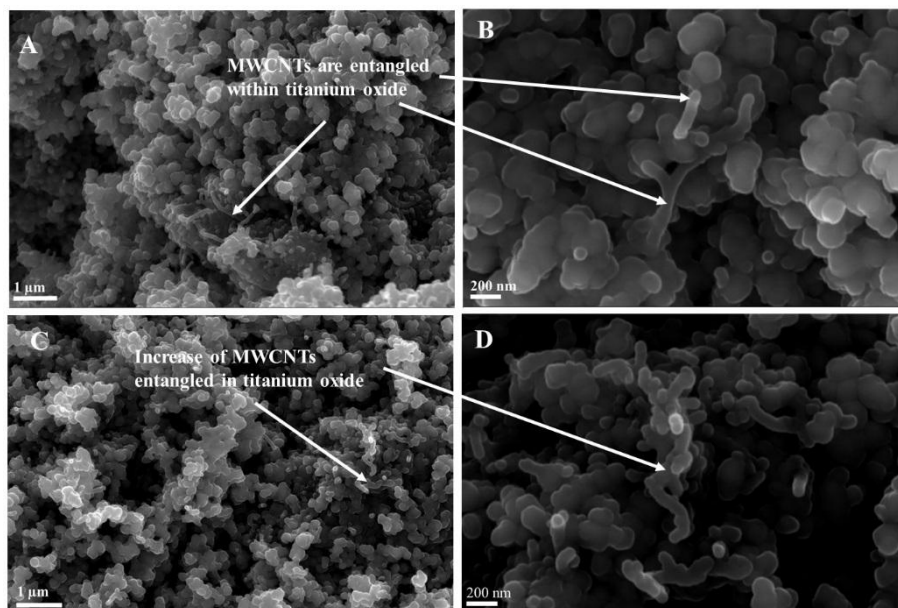


**Figure 2:** SEM images of admixed 1 wt. % MWCNTs in titanium oxide at lower magnification left and higher magnification right. A-B (6 hours) and C-D (9 hours).

Similarly, the SEM images of the admixed powder containing 1 wt. % MWCNTs in TiO<sub>2</sub> after milling for 6 and 9 hours at speed of 100 rpm is shown in figure 2. The SEM images shows figure 2A&C, B&D at lower magnification and higher magnification respectively. It was observed that MWCNTs were well dispersed as the milling time increases, an interlocking behaviour between the TiO<sub>2</sub> powder and MWCNTs was also observed and this could as a result of the bonding strength between MWCNTs and TiO<sub>2</sub> particles. Consequently, this was further revealed at higher

magnification where the MWCNTs expands in diameter in comparison to the as-received and this could be ascribed to the good bonding strength which was formed as a result of lengthy milling time.

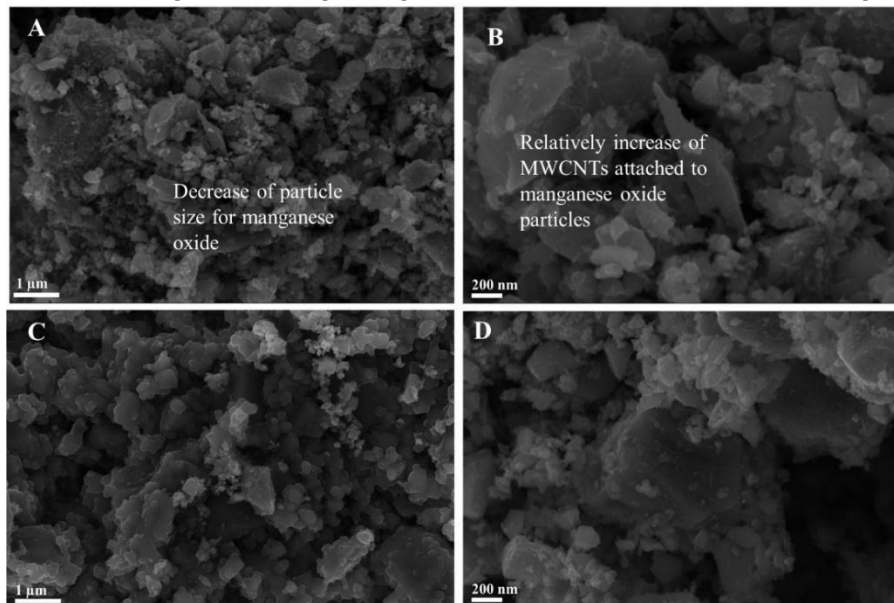


**Figure 3:** SEM images of admixed 1 wt. % MWCNTs in MnO<sub>2</sub> at lower magnification left and higher magnification right. A and B (6 hours) and C-D (9 hours).

Likewise, similar milling parameters were used in the dispersion of 1 wt. % MWCNTs in MnO<sub>2</sub> as shown in figure 3. From the SEM image (figure 3A), it was observed that the MWCNTs were relatively clustered on the surface of the MnO<sub>2</sub> particles. Due to the increase in milling time at lower magnification (figure 3C), it was observed that MWCNTs detangled to an extent at the same time reducing the MnO<sub>2</sub> particle sizes. At higher magnification (figure 3D) the images show the increase of the MWCNTs which was slightly dispersed on the surface of MnO<sub>2</sub> oxide particles. This could be due to longer milling time where higher energy was exerted to overcome the Van Waals forces and detangle MWCNTs.

The TEM images of MWCNTs/TiO<sub>2</sub> composite materials were shown in figure 4. In figure (4A), the TiO<sub>2</sub> particles clumped together around MWCNTs, while in figure (4C), which shows the TEM image of the 6 hours milled MWCNTs/TiO<sub>2</sub>, the MWCNTs were embedded within the crystalline structure of the TiO<sub>2</sub> and there no sign of wall deformation. It was also observed that an increase of milling time in figure (4G) revealed uniformly distribution of the MWCNTs, however, there was a deformation on the wall of the MWCNTs. These deformed walls can lead to the formation of non-sp<sup>2</sup> C-C defects which are potential sites for interfacial reaction [16].

Consequently, the above TEM images in figure 5 shows the MWCNTs/ MnO<sub>2</sub> composite that was conducted with similar milling parameters as MWCNTs/TiO<sub>2</sub>. It was shown that amorphous MnO<sub>2</sub> particles are clustered around the MWCNTs at figure (5A), however as the milling time increased in figure (5D) the dispersion of MWCNTs was observed alongside with size reduction of MnO<sub>2</sub> particles and this was ascribed to the lengthy milling time which was complimentary to the SEM images. Additionally, the HRTEM in figure (6C & F), shows slightly deformation of their walls, however with increase in milling time, the MWCNTs walls were highly deformed

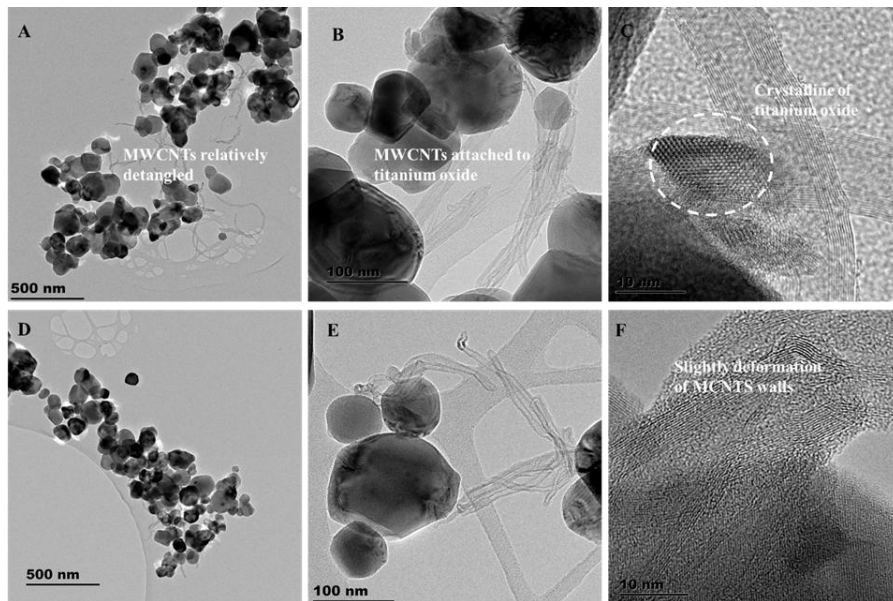


**Figure 4:** TEM images of admixed 1 wt. % MWCNTs in titanium oxide with varied milling time A-C (6 hours), D-F (9 hours).

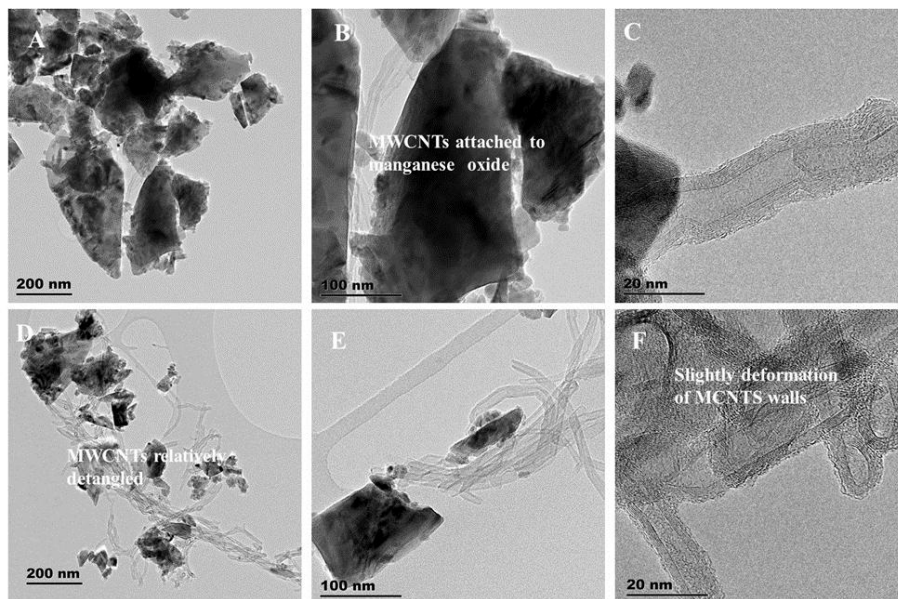


**Figure 5:** TEM images of admixed 1 wt. % MWCNTs in manganese oxide with varied milling time A-C (6 hours), C-D (9 hours).

### 3.2. Phase Analysis of the CNTs in transition metal oxides

X-ray diffraction techniques was utilized to identify the various phases, structural changes and the evolution of the crystalline phases in the as-received and admixed powders. Figure 6 shows the XRD patterns of as-received and admixed powders. The peaks observed located at 25.6 and 42.4 are possibly identified to the reflection from the (002) and (100) planes of MWCNTs. Due to addition of MWCNTs to the TiO<sub>2</sub>, the peaks observed are as follows; 25.41, 37.94, 48.2, 54.2, 55.3, 62.96, 69.02, 70.53, 75.30 and 82.55 which corresponds to (101), (004), (200), (105), (211), (204), (116), (116), (220), (215) and (303) of anatase TiO<sub>2</sub> powder. The MWCNTs (002) reflection overlaps the anatase TiO<sub>2</sub> (101) reflection in the MWCNTs/ TiO<sub>2</sub> composite. It was also observed that (101) peak slightly decreases with increase of milling time from which indicates that the MWCNTs are interlocked within TiO<sub>2</sub>. There are no other phases observed which indicates that the composite materials were well crystallised [17]

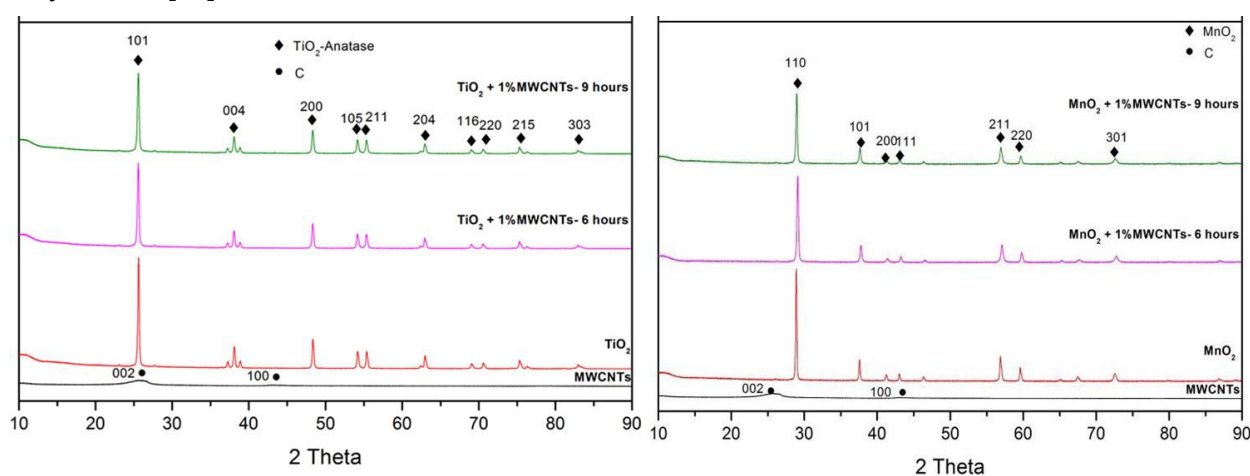


**Figure 6:** XRD patterns of titanium oxide and MWCNTs/ titanium oxide milled at different times (Left) and manganese oxide and MWCNTs/ manganese oxide milled at different times (Right).

Figure 6 (right) shows XRD patterns of MWCNTs and MWCNTs/MnO<sub>2</sub> composite material. As shown below at 25.6 and 42.4 could be the reflection from the (002) and (100) planes of MWCNTs. The major diffraction peaks which appeared as follows; 28.9, 37.6, 56.9 matched with diffraction peaks of (110), (101) and (211). The MWCNTs/MnO<sub>2</sub> XRD pattern showed that manganese oxide peaks were observed while the diffraction peaks from the MWCNTs were not obvious due to the uniform coating of the MWCNTs by MnO<sub>2</sub> layer [10]. This is complimentary with the SEM and TEM images where the increase of milling time enhanced the dispersion of MWCNTs and bonding to the MnO<sub>2</sub> particles surfaces.

## 4. Conclusion

In conclusion, the dispersion of MWCNTs in titanium and manganese oxide using HEBM technique became successful. The increase of milling time also increases the dispersion of MWCNTs in titanium and manganese oxide. However, it was observed that the irregular particles of manganese oxide powder promote the tendencies for size reduction of its particles and better dispersion of MWCNTs than titanium oxide. This is obvious on the SEM and TEM results where MWCNTs were relatively dispersed on the surfaces of the manganese oxide and with increase in milling time, the particles of manganese oxide were disintegrated. In addition, the harsh ball milling conditions of the HEBM created structural disorders such as non-sp<sup>2</sup> defects in the form of open edges on the sidewalls and vacancies in C–C system of MWCNTs.

## Acknowledgements

I would like to thank the National Research Foundation of South Africa for their financial support.

## References

- [1] Gupta V, Saleh TA. Syntheses of carbon nanotube-metal oxides composites; adsorption and photo-degradation, *InTech*; 2011.
- [2] Hu Y, Guo C. Carbon nanotubes and carbon nanotubes/metal oxide heterostructures: synthesis, characterization and electrochemical property, *InTech*; 2011.
- [3] Zhou H, Zhang L, Zhang D, Chen S, Coxon PR, He X, et al. A universal synthetic route to carbon nanotube/transition metal oxide nano-composites for lithium ion batteries and electrochemical capacitors. *Sci Rep* 2016;**6**:1–11. doi:10.1038/srep37752.
- [4] Li J, Tang S, Lu L, Zeng HC. 2007-Preparation of Nanocomposites of Metals , Metal Oxides , and Carbon Nanotubes via Self-Assembly.pdf 2007;**2**:9401–9.
- [5] Munir KS, Wen C. Deterioration of the Strong sp<sup>2</sup> Carbon Network in Carbon Nanotubes during the Mechanical Dispersion Processing—A Review. *Crit. Rev. Solid State Mater. Sci.* 2016;**41**:347–66.
- [6] Ajiteru OA, Tshephe TS, Okoro AM, Olubambi PA, Lephuthing S, Lesufi M. Evaluation of the methods of dispersion of carbon nanotubes (CNTs) in titanium and its alloys: Literature review. *Mech. Intell. Manuf. Technol. (ICMIMT)*, 2018 IEEE 9th Int. Conf., IEEE; 2018, p. 50–3.
- [7] Machaka R. Effects of Carbon Nanotubes on the Mechanical Properties of Spark Plasma Sintered Titanium Matrix Composites-A Review *n.d.*
- [8] Datsyuk V, Kalyva M, Papagelis K, Parthenios J, Tasis D, Siokou A, Chemical oxidation of multiwalled carbon nanotubes. *Carbon N Y* 2008;**46**:833–40. doi:10.1016/j.carbon.2008.02.012.
- [9] Sun Z, Yuan H, Liu Z, Han B, Zhang X. A highly efficient chemical sensor material for H<sub>2</sub>S:  $\alpha$ -Fe<sub>2</sub>O<sub>3</sub> nanotubes fabricated using carbon nanotube templates. *Adv. Mater.* 2005;**17**:2993–7.
- [10] Schlecht U, Balasubramanian K, Burghard M, Kern K. Electrochemically decorated carbon nanotubes for hydrogen sensing. *Appl. Surf. Sci.* 2007;**253**:8394–7.
- [11] LeeáTan K. Growth of Pd, Pt, Ag and Au nanoparticles on carbon nanotubes. *J. Mater. Chem.* 2001;**11**:2378–81.
- [12] Munir KS, Qian M, Li Y, Oldfield DT, Kingshott P, Zhu DM, et al. Quantitative Analyses of MWCNT-Ti Powder Mixtures using Raman Spectroscopy: The Influence of Milling Parameters on Nanostructural Evolution. *Adv. Eng. Mater.* 2015;**17**:1660–9.
- [13] Ci L, Ryu Z, Jin-Phillipp NY, Rühle M. Investigation of the interfacial reaction between multi-walled carbon nanotubes and aluminum. *Acta Mater.* 2006;**54**:5367–75.
- [14] Ebbesen TW, Ajayan PM. Large-scale synthesis of carbon nanotubes. *Nature* 1992;**358**:220.
- [15] Ajayan PM, Ebbesen TW. Nanometre-size tubes of carbon. *Reports Prog. Phys.* 1997;**60**:1025.
- [16] Munir KS, Zheng Y, Zhang D, Lin J, Li Y, Wen C. Microstructure and mechanical properties of carbon nanotubes reinforced titanium matrix composites fabricated via spark plasma sintering. *Mater Sci Eng A* 2017;**688**:505–23. doi:10.1016/j.msea.2017.02.019.
- [17] Kiamahalleh MV, Najafpour G, Abd SS, Buniran S, Zein SHS. Multiwalled carbon nanotubes filled with transition metal oxides as supercapacitor materials. *World Appl. Sci. J.* 2010;**9**:1–7.